RESEARCH ARTICLE

# Ultrastructural and quantitative analysis of the lipid droplet clustering induced by hepatitis C virus core protein

**Marion Depla · Rustem Uzbekov · Christophe Hourioux ·
Emmanuelle Blanchard · Amélie Le Gouge ·
Ludovic Gillet · Philippe Roingeard**

**Abstract** Hepatitis C virus (HCV) release is linked to the formation of lipid droplet (LD) clusters in the perinuclear area of infected cells, induced by the core protein. We used electron microscopy (EM) to monitor and compare the number and size of LD in cells producing the mature and immature forms of the HCV core protein, and 3D EM to reconstruct whole cells producing the mature core protein. Only the mature protein coated the LD and induced their clustering and emergence from endoplasmic reticulum membranes enriched in this protein. We found no particular association between LD clusters and the centrosome in reconstructed cells. The LD clustering induced by the mature core protein was associated with an increase in LD synthesis potentially due, at least in part, to the ability of this protein to coat the LD. These observations provide useful information for further studies of the mechanisms involved in HCV-induced steatosis.

M. Depla · R. Uzbekov · C. Hourioux · E. Blanchard ·
P. Roingeard (✉)
INSERM U966, Faculté de Médecine, Université François Rabelais, CHRU de Tours, 10 boulevard Tonnellé, 37032 Tours Cedex, France
e-mail: roingeard@med.univ-tours.fr

A. Le Gouge
INSERM CIC 0202, Université François Rabelais, CHRU de Tours, Tours Cedex, France

L. Gillet
INSERM U921, Université François Rabelais, CHRU de Tours, Tours Cedex, France

**Abbreviations**

| | |
|---|---|
| HCV | Hepatitis C virus |
| ER | Endoplasmic reticulum |
| SPP | Signal peptide peptidase |
| SFV | Semliki forest virus |
| EM | Electron microscopy |
| $\beta$-Gal | $\beta$-Galactosidase |
| WT | Wild-type |

## Introduction

Hepatitis C virus (HCV), a member of the Flaviviridae family, is a major cause of chronic liver disease, infecting an estimated 170 million people worldwide [1]. The spectrum of severity of the liver disease associated with HCV is broad and the rate of progression to advanced fibrosis and cirrhosis is highly variable. This rate seems to depend on many host-related cofactors, such as age at infection, sex, alcohol consumption, being overweight and co-infections with hepatitis B virus or human immunodeficiency virus [2]. Retrospective studies have shown that advanced fibrosis is associated with the presence and severity of liver steatosis, characterised by the deposition of triglycerides in the liver [3, 4]. There is, therefore, considerable interest in dissecting the mechanisms of steatosis in HCV infection, particularly in relation to other metabolic disturbances. Steatosis is frequent in hepatitis C patients. Indeed, before the advent of serological testing, the presence of fatty acids in the liver was widely considered to be suggestive of a diagnosis of non-A, non-B

hepatitis [5]. Steatosis depends on both viral and host factors. Virus-induced steatosis is mostly reported in patients infected with HCV genotype 3, in whom fat accumulation is correlated with HCV replication in the serum [3] and liver [6], and is resolved by successful antiviral treatment [7, 8], strongly suggesting that specific viral products are involved in the fat deposition. By contrast, most cases of mild steatosis in patients infected with genotypes other than 3 seem to have a metabolic pathogenesis, with being overweight identified as the most significant clinical correlate [3]. This type of steatosis tends to be associated with a lower likelihood of virological response to antiviral drugs [9] and frequently persists in patients responding to antiviral treatment, consistent with HCV playing no major role in its pathogenesis [8, 9]. Both types of steatosis (viral and metabolic) may co-exist in at least some chronic hepatitis C patients, although steatosis is more likely to be predominantly viral in origin in patients infected with genotype 3 viruses and predominantly metabolic in patients infected with viruses of other genotypes.

The HCV genome consists of a positive-sense, single-stranded RNA molecule of 9.6 kb [10]. Translation of the genome generates a polyprotein of approximately 3,000 amino acids, which is cleaved by a combination of viral and cellular proteases to produce the mature structural and non-structural proteins. The structural protein involved in nucleocapsid assembly—the core protein—has been shown to induce steatosis in two lines of transgenic mice [11, 12]. HCV core protein production is associated with multiple changes in lipogenic gene expression [13–16] and lipogenic proteins activity [17, 18], and also has effects on mitochondrial oxidative function [19–21]. In vitro studies on various cell lines rapidly established that the HCV core protein was located at the surface of lipid droplets acting as intracellular storage sites for triglycerides and cholesterol esters [22–25]. Moreover, HCV core has been shown to be present on lipid droplets in liver biopsy specimens from infected chimpanzees [23]. These observations raise the intriguing possibility that this particular localisation is somehow linked to liver steatosis [26]. Recent fundamental research studies made possible by the isolation of a virus strain (JFH-1, Japanese Fulminant Hepatitis clone 1) producing infectious HCV from tissue culture cells have demonstrated that the initiation of nascent virions assembly and production takes place at lipid droplets [27]. Indeed, attachment of the HCV core protein to lipid droplets is linked to the release of infectious progeny virions from infected cells. This release is accompanied by the redistribution of lipid droplets within infected cells, with the clustering of these lipid droplets in the perinuclear area [28]. This redistribution requires only the mature HCV core protein, generated by cleavage with two cellular enzymes: signal peptidase and signal peptide peptidase (SPP). The

first of these enzymes releases the core protein from the polyprotein targeted to the endoplasmic reticulum (ER) membrane, generating an immature form of the core protein that contains the signal peptide [29]. Complete processing of the protein requires further proteolysis by SPP, which cleaves within the signal peptide. This second cleavage event is essential for the trafficking of the core protein to the lipid droplet [29]. The redistribution of lipid droplets induced by the mature HCV core protein depends on the microtubule network and is thought to increase the likelihood of interaction between the core protein and the site of HCV RNA replication within a network of membranes in the perinuclear area [28]. Thus, the association of the HCV core protein with lipid droplets seems to play a central role in both HCV pathogenesis and morphogenesis, suggesting that virus-induced steatosis may be essential for the viral life cycle.

We have previously established a cellular model based on HCV core protein production in which lipid droplets accumulate and cluster in the perinuclear area of the transfected cells [30]. Using this model, together with a new method for monitoring the number and size of lipid droplets in transfected cells, we demonstrated that the production of a core protein bearing residues specific to HCV genotype 3 was associated with a higher amount of lipid droplets than the production of a wild-type (WT) core protein of genotype 1 [30]. Thus, our cellular model seems to mimic, in vitro, virus-induced steatosis and its genotype-specific influence. In this study, we used this model to compare the amount of intracellular lipid droplets in cells producing immature and mature HCV core proteins. We also analysed the clustering of lipid droplets induced by the mature HCV core protein, by 3D electron microscopy, and considered the implication of these observations for the potential mechanisms underlying HCV-induced steatosis.

## Materials and methods

### Insertion of the HCV core sequences into Semilki forest virus (SFV) vectors and site-directed mutagenesis to generate an HCV core mutant not cleaved by SPP

The HCV core 1a construct was obtained from our previously described [31] genotype 1a cDNA clone (Dj6.4; Genbank accession number AF529293) containing the C-E1–E2 coding sequence. The WT core construct was amplified by PCR, using *PfuTurbo* DNA polymerase (Stratagene, La Jolla, CA, USA) with primers flanked by *Bam*H1 sites, as previously reported [32]. Site-directed mutagenesis within the C-terminal core signal sequence was performed with antisense primers leading to (1) the generation of a triple mutant VLV$^{180-3-4}$ (Fig. 1a) and (2)
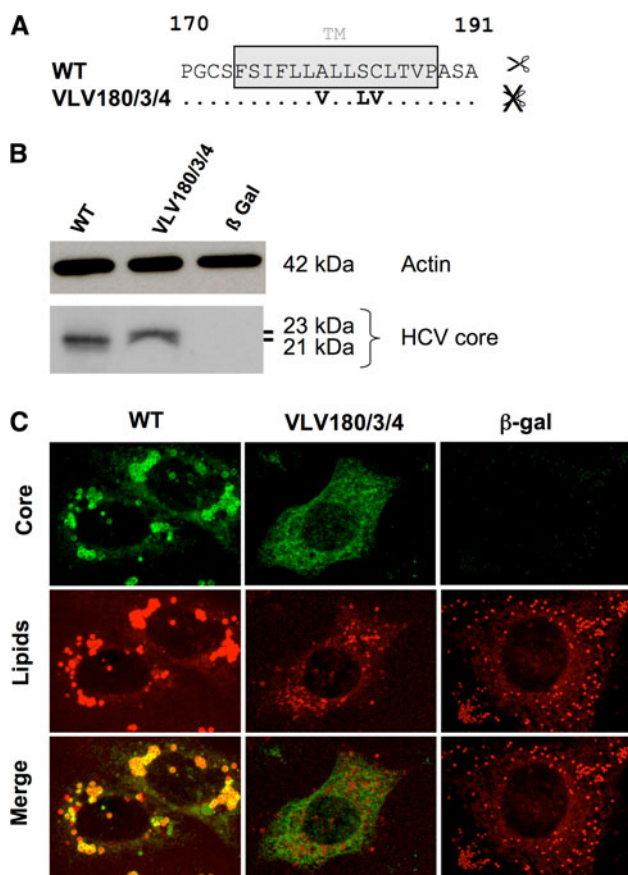
**Fig. 1** Analysis of HCV core protein production and core-E1 signal peptide processing. **a** Signal sequences of the two HCV core proteins used in this study: the wild-type (*WT*) protein and the $VLV^{180-3-4}$ mutant. The transmembrane region of the signal sequence at the core-E1 junction is *boxed*. **b** Production of the *WT* and $VLV^{180-3-4}$ mutant core proteins in BHK-21 cells, and analysis of HCV core protein processing by SDS-PAGE and western blotting. The WT core protein was fully cleaved by SPP, appearing at 21 kDa, whereas the $VLV^{180-3-4}$ mutant core protein remained uncleaved, resulting in detection of the p23 kDa form of the core protein. Cells producing *β-gal* were used as a control and an anti-actin antibody was used to normalise the western blot. **c** Immunofluorescence of *WT* and $VLV^{180-3-4}$ core proteins, combined with Nile Red staining of lipid droplets in FLC4 cells. Lipid droplets were evenly distributed throughout the cytoplasm of cells producing *β-gal* (negative control). Significant clusters of lipid droplets co-localised with core protein were observed in the perinuclear area of cells transfected with the WT core construct, but not in cells producing the $VLV^{180-3-4}$ mutant core

the insertion of a stop codon at the 3′ end of the core protein-coding region [33]. This particular mutant has been shown to be resistant to SPP cleavage [33]. The sequences encoding the WT and mutated core proteins were inserted separately into the polylinker *Bam*H1 site of the expression vector pSFV1 (Life Technologies, Rockville, MD, USA). DNA sequencing was used to check that the original sequence was conserved in both constructs and that the $VLV^{180-3-4}$ mutations were correctly introduced in the mutant.

Cell culture and transfection with RNA

Baby hamster kidney cells (BHK-21) were cultured and electroporated with recombinant SFV RNA encoding the HCV WT or $VLV^{180-3-4}$ core protein, as previously described [30, 33]. Briefly, cells were cultured at 37°C in Glasgow Minimal Essential Medium (GMEM) supplemented with 5% foetal calf serum and 8% tryptose phosphate. For recombinant RNA synthesis, the various pSFV1 constructs were linearised by digestion at the *Spe*I restriction site downstream from the 3′ non-coding region of the SFV replicon. Transcription was then carried out in vitro with SP6 RNA polymerase, making use of the SP6 promoter located upstream from the 5′ extremity of the SFV replicon, as recommended by the manufacturer (Invitrogen). As a control, we synthesised a recombinant RNA encoding β-galactosidase (β-Gal). For transfection, $10 \times 10^6$ cells were mixed with 5 µg of recombinant SFV RNA and electroporated by a single pulse at 350 V, 750 mF (Easyject One; Eurogentec). Cells were cultured for 16 h following electroporation, as our previous studies have shown that the major morphological events associated with HCV structural protein production occur during this period in this system [30, 33]. All experiments other than confocal microscopy studies of the subcellular distribution of core proteins were conducted with BHK-21 cells. For these confocal microscopy studies, we transfected the human hepatocellular carcinoma cell line FLC4 under similar conditions. The lower efficiency of the SFV vectors in these cells resulted in the production of smaller amounts of protein than in BHK-21 cells, allowing a more precise analysis of the subcellular distribution of proteins and an analysis of co-localisation with lipids [30, 33].

Western blotting

Transfected BHK-21 cells were treated with a lysis buffer containing 1% NP-40, 140 mM NaCl, 100 mM Tris–HCl pH 8, 1% sodium deoxycholate, 0.1% sodium dodecyl sulphate, 1 mM phenylmethylsulfonyl fluoride, 2 µg/ml aprotinin and 2 µg/ml leupeptin. Samples were then separated by SDS-PAGE in 15% polyacrylamide gels and the resulting bands were transferred to a polyvinylidene difluoride membrane. The membrane was blocked by incubation in 0.05% (vol/vol) Tween 20 in phosphate buffered saline (PBS) supplemented with 2% (wt/vol) skimmed milk powder (PBS-T). Membranes were incubated with the human monoclonal anti-HCV core B12F8 antibody (gift of Dr M. Mondelli) diluted 1:500 in PBS-T, washed and incubated with a horseradish peroxidase-conjugated anti-human antibody diluted 1:5,000 in PBS-T. Antibody binding was detected by enhanced chemiluminescence (ECL Plus; Amersham Bioscience).

## Confocal microscopy

Transfected FLC4 cells were cultured on glass coverslips for 16 h and were then fixed by incubation for 30 min in 4% paraformaldehyde in PBS at room temperature. The reaction was quenched and the cells were permeabilised by incubation for 30 min in 0.05% saponin-0.2% bovine serum albumin (BSA) in PBS. HCV core proteins were detected by incubating the cells for 30 min with the mouse monoclonal anti-HCV core antibody C7-50 (Abcam, Cambridge, MA, USA), diluted 1:100 in permeabilisation buffer. The cells were then washed and incubated with a secondary anti-mouse antibody coupled to Alexa Fluor 488 (Molecular Probes, Eugene, OR, USA), diluted 1:1,000 in permeabilisation buffer. For lipid staining, the cells were treated with Nile Red (Sigma-Aldrich), diluted 1:1,000 (from a 1 mg/ml stock solution in acetone) in permeabilisation buffer, during incubation with the secondary antibody. Confocal microscopy was performed with an Olympus Fluoview 500 instrument.

## Electron microscopy and immuno-electron microscopy

For standard electron microscopy (EM), transfected BHK-21 cells were fixed by incubation for 48 h in 4% paraformaldehyde and 1% glutaraldehyde in 0.1 M phosphate buffer (pH 7.2) and postfixed by incubation for 1 h with 2% osmium tetroxide (Electron Microscopy Science, Hatfield, PA, USA). They were dehydrated in a graded series of ethanol solutions, cleared in propylene oxide, and embedded in Epon resin (Sigma), which was allowed to polymerise for 48 h at 60°C. Ultrathin sections were cut, stained with 5% uranyl acetate, 5% lead citrate, and placed on EM grids coated with collodion. The sections were then observed with a Jeol 1230 transmission electron microscope (Tokyo, Japan) connected to a Gatan digital camera driven by Digital Micrograph software (Gatan, Pleasanton, CA, USA) for image acquisition and analysis. For immuno-EM, transfected BHK-21 cells were fixed by incubation in a solution containing 4% paraformaldehyde in 0.1 M phosphate buffer (pH 7.2) for 16 h. The cells were collected by centrifugation and the cell pellet was then dehydrated in a graded series of ethanol solutions at −20°C, using an automatic freezing substitution system (AFS; Leica), and embedded in London resin white (Electron Microscopy Science). The resin was allowed to polymerise at −25°C, under UV light, for 72 h. Ultrathin sections were cut and blocked by incubation with 1% fraction V bovine serum albumin (BSA; Sigma) in PBS. They were then incubated with anti-HCV core C7-50 monoclonal antibody diluted 1:50 in PBS supplemented with 1% BSA, washed and incubated with goat anti-mouse

antibodies conjugated to 15 nm gold particles (British Biocell International, Cardiff, UK) diluted 1:40 in PBS supplemented with 0.1% BSA. We used conjugated goat secondary antibodies without prior incubation with primary antibody to check that the reaction was specific. Ultrathin sections were stained and observed as described above.

## Lipid droplet quantification and statistical analysis

We used our recently established method for morphometric analysis of the lipid droplets encountered in cells [30]. Briefly, for each construct ($\beta$-Gal, WT core, VLV$^{180-3-4}$ core mutant), the number and diameter (in μm) of lipid droplets were determined on the computer screen for 100 consecutive EM (standard) sections of the transfected BHK-21 cells. Lipid droplet diameter was converted into an area in μm$^2$. By summing these areas, we were able to determine the cumulative lipid droplet area, in μm$^2$, for each cell section. Lipid droplet areas in 100 consecutive EM sections of the transfected cells seemed to follow mixed distributions. Indeed, the probability of observing a null area (discrete component of the distribution) was non-null, whereas a probability density function existed for all non-zero values of cumulative areas (continuous component of the distribution). We therefore categorised the variable before carrying out statistical tests. Based on Sturges' rule, we defined seven classes of cumulative lipid droplet area (0, 0–0.25, 0.25–0.5, 0.5–1, 1–1.5, 1.5–2 and 2–4 μm$^2$), thereby defining an ordinal variable. Constructs were compared by chi-squared test for trend taking into account the ordinal nature of the newly created variables. We also considered the proportion of cell sections with null area which were compared by a chi-squared test. Data were analysed with SAS 9.1 software.

## Triglyceride quantification

Ten millions of BHK-21 cells transfected with recombinant SFV RNA encoding the HCV WT, VLV$^{180-3-4}$ core protein or $\beta$-galactosidase were collected in 1 mL of PBS. Total lipids extraction was performed using a method adapted from Folch et al. [34]. Briefly 3 mL of a 2:1 chloroform–methanol (v/v) mixture and 1 mL water were added to 1 mL of cell suspension. After homogenisation and centrifugation the resulting mixture separated into two phases. The lower phase containing total lipids was collected, then evaporated, and lipids were dissolved in isopropanol. Triglyceride concentration was then measured by enzymatic reaction using the colorimetric kit TG PAP 150 (BioMérieux, Marcy l'Etoile, France). Data were displayed with the $\beta$-galactosidase as control (test/control ratio of the optic density values).

### Three-dimensional (3D) reconstruction analysis of whole cells producing the WT HCV core protein

We have recently described the use of serial EM sections for the 3D reconstruction of large cellular microdomains in cells producing the HCV core protein [35]. This previous study demonstrated that the budding of the HCV-like particles formed by self-assembly of the HCV core protein was initiated mostly at ER membranes closely associated with lipid droplets [34]. In this study, we used a similar approach to reconstruct several whole BHK-21 cells producing the WT HCV core protein. Briefly, we resized our Epon blocks to cut a ribbon of serial ultrathin sections (75 nm thick) of transfected cells. EM grids were stained as described above, and electron micrographs were collected with a digital camera for the same region of cells in each of the series of sections. Photoshop software was used to align image stacks for these serial EM sections. As the electron beam distorts ultrathin sections slightly, it was necessary to align the images based on the position of specific structures of interest. Contours were carefully drawn with IMOD software [36] through the same specific cellular structures on different serial sections. These structures included the plasma membrane, nuclear envelope, lipid droplets and centrosome. The contours from a stack of serial sections were then arranged into objects with IMOD. Using the IMODmesh feature of IMOD, we then joined the contours of each object to form a 3D model. Nine cells were analysed thoroughly to determine the subcellular distribution of their lipid droplets. A lipid droplet cluster was defined as at least three droplets grouped together, with the individual droplets of the cluster separated by less than the mean diameter of a lipid droplet (i.e. 0.5 μm). A lipid droplet cluster was considered to be closely associated with a centrosome if at least one lipid droplet from the cluster was less than 1.5 μm from the nearest centriole.

## Results

### Expression and processing of HCV WT core and VLV$^{180-3-4}$ core mutant proteins

Sixteen hours after transfection with the constructs encoding HCV core proteins or the β-gal control, the cells were harvested and lysed for western blot analysis (Fig. 1b). Consistent with our previous findings [30–33], the WT core protein encoded by the Dj6.4 sequence appeared to be fully cleaved by SPP, leading to the detection of a p21 protein, whereas the VLV$^{180-3-4}$ core mutant remained uncleaved, resulting in the detection of a p23 form of the core protein. We used Image J software for gel analysis to quantify the WT and mutant core proteins in the scanned blot and found that these two proteins were present in similar amounts.

### Colocalisation of HCV core proteins with lipid droplets

Nile Red labelling in cells transfected with the β-gal construct showed that lipid droplets were evenly distributed throughout the cytoplasm (Fig. 1c). Transfection with the WT core construct induced the clustering of large lipid droplets in the perinuclear area, as previously reported for our model [30, 33] and for other in vitro cellular models [28]. The surface of these droplets was strongly stained for HCV core protein, as previously described in these models [28, 30, 33]. Transfection with the VLV$^{180-3-4}$ core mutant construct did not induce lipid droplet clustering, and this mutant core protein displayed only a weak association with lipids, which were evenly distributed throughout the cytoplasm, as previously described [33]. Similar results were obtained when the experiment was repeated and for analyses of large numbers of cells (only one cell is shown for each construct in Fig. 1c, to show the colocalisation of HCV core proteins and lipid droplets as clearly as possible).

### Electron microscopy and immuno-electron microscopy

Standard electron microscopy showed that the ultrastructural changes observed in cells transfected with recombinant SFV vectors encoding the WT core protein were consistent with our previous findings [30, 33], with the clustering of large lipid droplets in the perinuclear area (Fig. 2, top). These lipid droplet clusters were systematically surrounded by convoluted ER membranes rich in HCV-like particles budding towards the lumen of this convoluted ER compartment, as previously described (Fig. 2) [35]. Transfection with β-Gal RNA had no effect on ER morphology, with linear ER membranes evenly distributed throughout the cytoplasm (not shown). Immuno-electron microscopy on freeze-substituted cells producing the WT core protein showed that the surface of the clustered lipid droplets and their surrounding ER membranes stained strongly positive for HCV core protein (Fig. 2, bottom). Standard electron microscopy in cells transfected with the recombinant SFV RNA encoding the VLV$^{180-3-4}$ core mutant revealed multiple layers of dense ER membranes, as previously described [33] (Fig. 2, top). It has been suggested that this particular mutant, which is not processed by SPP and thus remains anchored in the ER membrane by its transmembrane sequence signal, induces these multi-layered ER membranes by protein–protein interaction [33]. This hypothesis was recently confirmed by another group [37]. Immuno-electron microscopy on freeze-substituted cells producing this mutant showed that
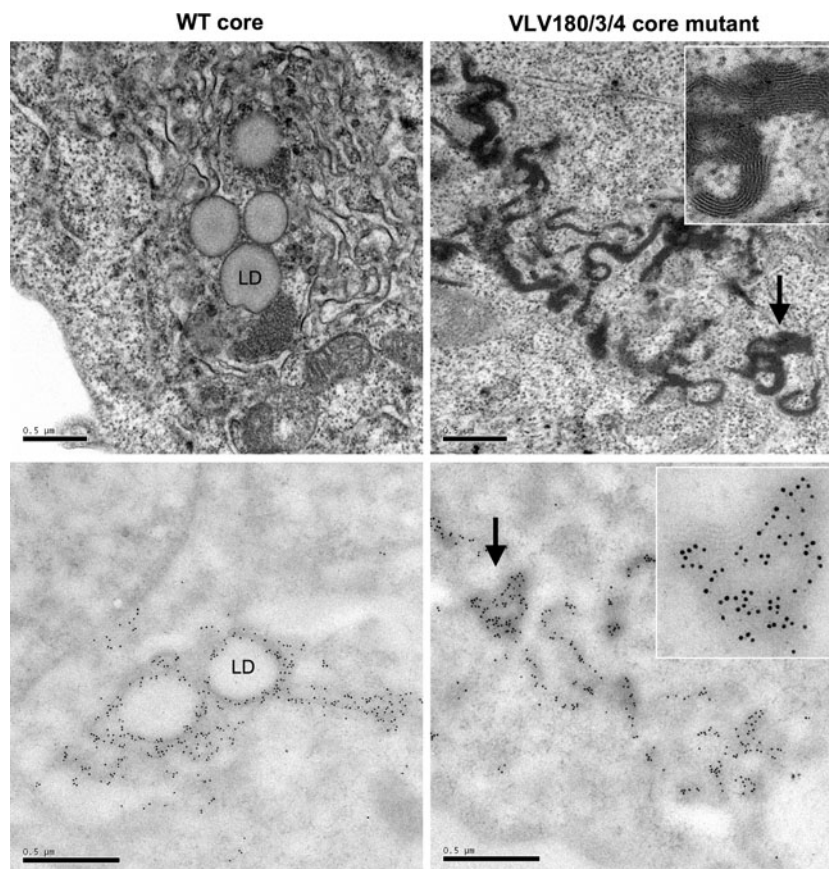
**Fig. 2** Electron micrographs of ultrathin sections of BHK-21 cells producing the WT core or VLV$^{180-3-4}$ core mutant protein studied by regular EM (*upper image*) or freeze substitution and immunogold labelling with a monoclonal anti-HCV core (*lower image*). Cells producing the WT core protein contained convoluted ER membranes surrounding clusters of lipid droplets (*LD*). These convoluted membranes surrounding the droplets and the surface of the droplets themselves stained strongly for the HCV core by immunogold labelling. Cells producing the VLV$^{180-3-4}$ core mutant contained abundant electron-dense, multi-layered structures formed by the interaction of multiple ER membranes (see also the *inset* corresponding to an enlargement of the area indicated by the *arrow*). These multi-layered ER membranes were strongly positive for the HCV core protein on immunogold labelling. No gold labelling was detected at the surface of the lipid droplets in these cells. All these structures were specific to the HCV core protein, as none of these modifications or immunogold labelling was detected in cells producing $\beta$-gal (data not shown). *Scale bars* 0.5 μm in all micrographs

these multi-layered ER membranes were strongly positive for HCV core protein (Fig. 2, bottom).

Lipid droplet quantification

We determined the cumulative area covered by lipid droplets for 100 consecutive cell sections, for each construct, studied in random order (Fig. 3). The cumulative area of the lipid droplets was higher for both core proteins than for the control protein $\beta$-gal ($p < 0.0001$ for the WT core protein; $p = 0.0029$ for the VLV$^{180-3-4}$ core mutant). This cumulative area was greater for the WT core protein than for the VLV$^{180-3-4}$ mutant core protein, although this difference was of low significance ($p = 0.0634$). However, the proportion of cell sections with null areas (thick lines in 0) was lower with the WT core protein than with the VLV 180/3/4 core mutant protein (respectively, 35 vs 56%, $p = 0.003$).
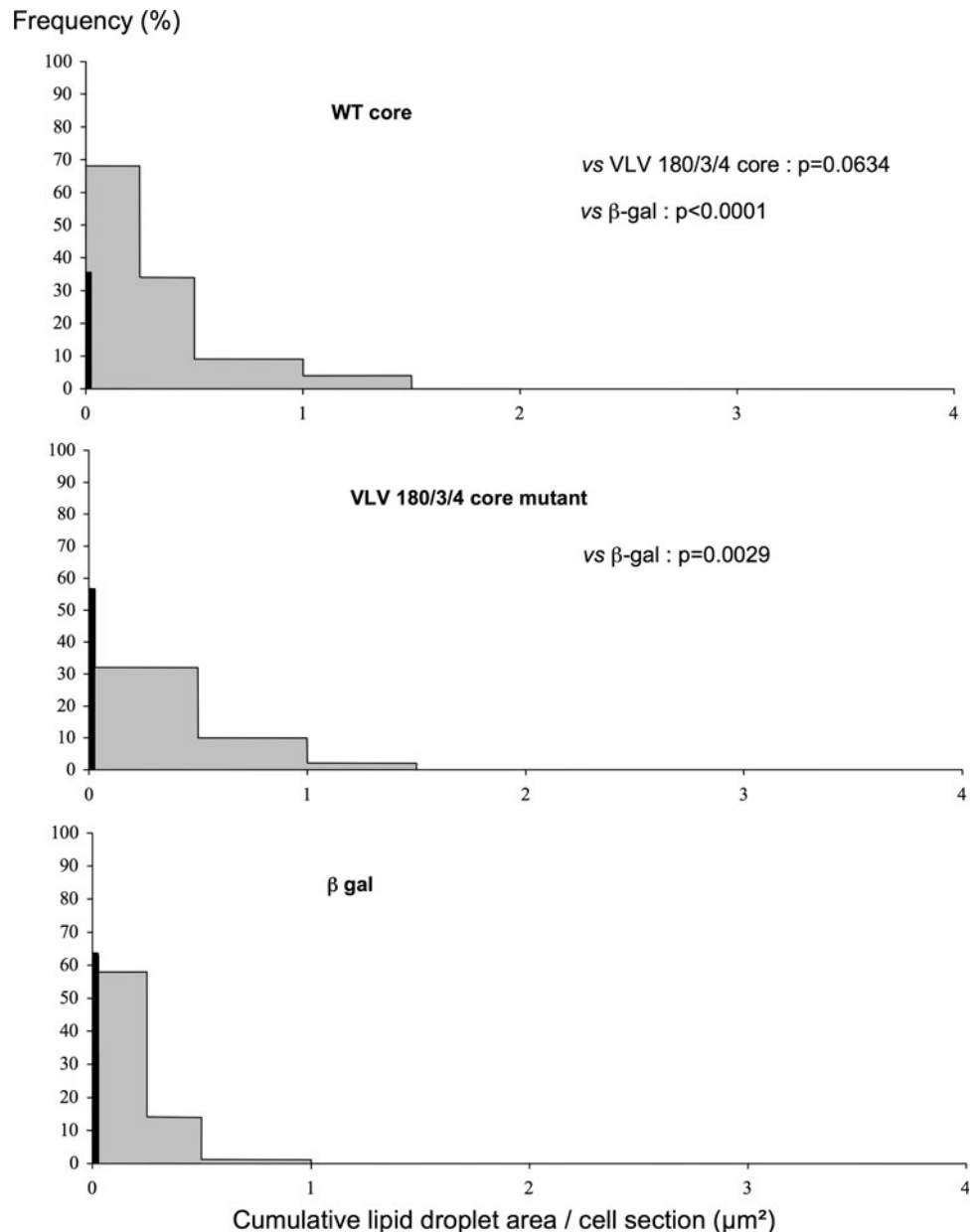
Triglyceride quantification

We measured the total amount of triglycerides in cells transfected with the various constructions, using a commercially available colorimetric assay. Triglyceride accumulation in cell producing the VLV$^{180-3-4}$ core mutant or the WT core protein was about 1.5-fold and 2.0-fold with respect to the control $\beta$-galactosidase protein, respectively (Fig. 4).

3D reconstruction analysis of whole cells producing the WT HCV core protein

Nine cells producing the WT core protein and containing at least one lipid droplet cluster were fully reconstructed in 3D with our method based on serial EM sections (between 150 and 180 sections for a typical cell). We considered a lipid droplet cluster to have formed when three of more

**Fig. 3** Quantification of the cumulative area covered by lipid droplets in sections of BHK-21 cells producing the WT core protein, the $VLV^{180-3-4}$ core mutant or the $\beta$-galactosidase control protein. The cumulative area covered by lipid droplets per cell section (in $\mu m^2$) was determined on 100 consecutive cell sections for each protein. The cumulative lipid droplet area was categorised into seven classes: 0, 0–0.25, 0.25–0.5, 0.5–1, 1–1.5, 1.5–2 and 2–4 $\mu m^2$. The probability distributions were mixed distributions. The *thick line* in 0 indicates the frequency of null areas, whereas non-null areas are presented as *histograms*. The chi-squared test associated with the comparison of the WT core with the $VLV^{180-3-4}$ core mutant or $\beta$-galactosidase yielded *p* values of 0.0634 and <0.0001, respectively. The chi-squared test associated with the comparison of $VLV^{180-3-4}$ core mutant with $\beta$-galactosidase yielded a *p* value of 0.0029

Frequency (%)

WT core

*vs* VLV 180/3/4 core : p=0.0634

*vs* β-gal : p<0.0001

VLV 180/3/4 core mutant

*vs* β-gal : p=0.0029

β gal

Cumulative lipid droplet area / cell section ($\mu m^2$)

lipid droplets were found in close proximity (less than the mean lipid droplet diameter, 0.5 μm, apart). We observed 1–4 lipid droplet clusters per cell in these nine cells and analysed 20 lipid droplet clusters in total. A lipid droplet cluster was considered to be associated with a centrosome when at least one of the lipid droplets of the cluster was found to be located less than 1.5 μm from the nearest centriole. Only 4 out of these 20 lipid droplet clusters observed were associated with a centrosome. In the cases in which only one lipid droplet cluster per cell was observed, the lipid droplet cluster concerned was never associated with the centrosome. Figure 5 illustrates a typical cell with a single large lipid droplet cluster, in which the centrosome is opposite the lipid droplet cluster within the cytoplasm

(see also the QuickTime movie of the 3D reconstruction of this cell in the electronic supplementary material, which illustrates the spatial distribution of these different organelles within the cell).

## Discussion

A recent study assessing the spatial dispersion of lipid droplets through the cytoplasm by confocal microscopy demonstrated that these organelles group together in clusters in the perinuclear area of HCV-infected cells [28]. Disruption of the microtubule network or the microinjection of dynein antibodies prevent the formation of these
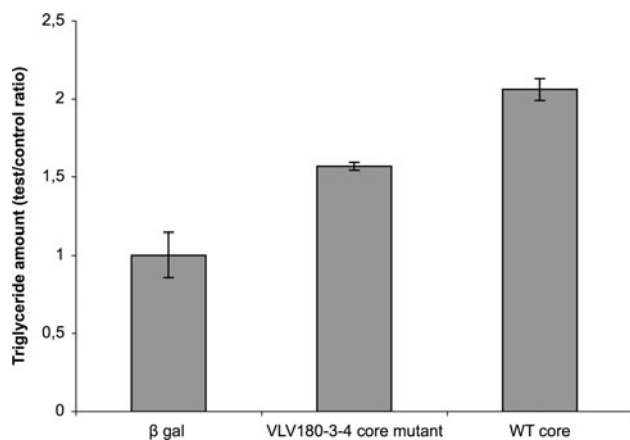
**Fig. 4** Triglyceride quantification in BHK-21 cells producing the WT core protein, the $VLV^{180-3-4}$ core mutant, or the $\beta$-galactosidase control protein, using a commercially available assay (Biomérieux). Data are displayed with the $\beta$-galactosidase as control (test/control ratio of the optic density values), and are mean $\pm$ standard deviations of four independent quantifications



**Fig. 5** Three-dimensional reconstruction of a BHK-21 cell producing the WT core protein. **a** Typical single ultrathin section of this cell, showing its centrosome (*arrow* and enlargement in the *inset*) distant from the cluster of lipid droplets (LD). *Bars* 2 μm. **b** Four different views of the reconstruction of this cell obtained with IMOD software and a total of 145 serial ultrathin (60–70 nm thick) EM sections, showing the plasma membrane (*light green*), the nucleus (*purple*), the centrosome (*light purple* and *arrow*) and the lipid droplets (*yellow*). The cluster of lipid droplets is located in a cellular domain opposite to the centrosome (*arrows*). A QuickTime movie of this 3D reconstruction is also provided in the electronic supplemental material

clusters, which are thought to occur specifically around the centrosome. The authors of this previous study interpreted these results as indicating a global redistribution of the pre-existing lipid droplets following HCV infection, through the trafficking of these organelles along the microtubule network and towards the centrosome. This phenomenon was observed in the hepatoma cell line Huh7 infected with the complete virus (the JFH-1 strain), and also in Huh7 cells producing only the mature HCV core protein of various genotypes [28]. An immature core protein (i.e. not cleaved by SPP) did not induce these specific clusters in the Huh7 cells and the lipid droplets therefore remained dispersed through the cytoplasm. This previous study was based on a system of core protein production from an SFV vector, resulting in the rapid induction of these lipid droplet clusters in 16 h, rather than 3 days required in cells infected with the complete virion [28]. To investigate this phenomenon further, we used here SFV vectors to produce the mature and immature core proteins in the BHK-21 cell line. This cell line was chosen for the high percentage of transfected cells (near 100%) reached after electroporation, allowing a better analysis of the changes induced by the core proteins in the lipid droplets amount. Moreover, this cell line has been previously shown to accumulate triglycerides in cytoplasmic lipid droplets [38]. We used different EM approaches such as immuno-EM, 3D reconstructions and EM for lipid droplet quantification. EM has been shown to be a more appropriate method than light microscopy for quantifying the lipid droplets within cells [35], and 3D EM reconstructions gave a more precise subcellular localisation of centrosomes and lipid droplets.

Our morphometric analysis of lipid droplets in cells transfected with the various constructs clearly shows that
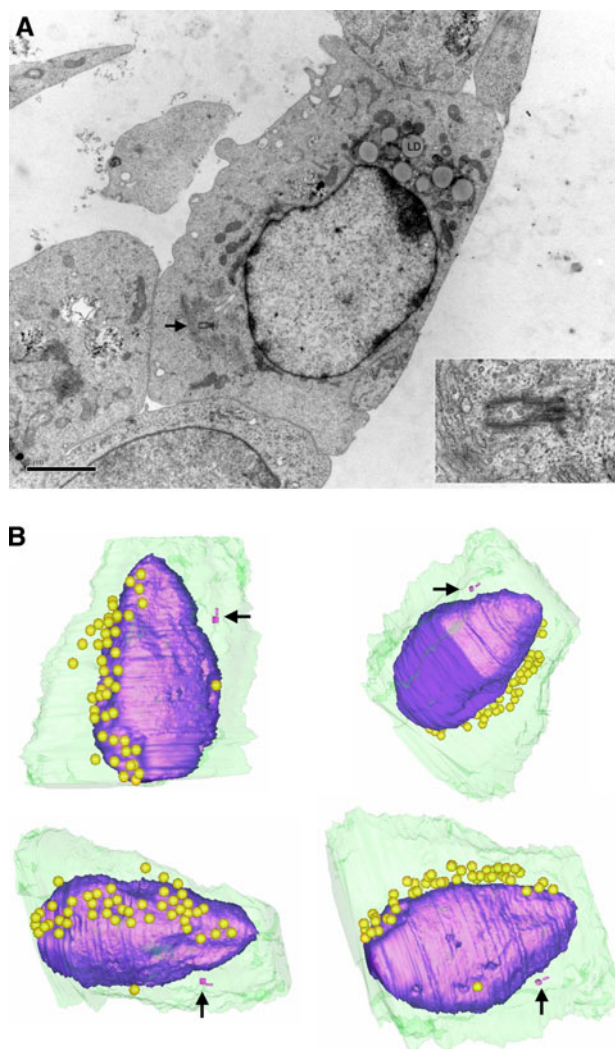
HCV core protein production is associated with a larger cumulative area being covered by lipid droplets. This greater area was observed for both the mature (WT) and immature (uncleaved mutant) forms of the HCV core protein. This was also supported by the quantification of the triglycerides in the transfected cells, showing an increase in triglyceride synthesis in cells producing the WT and mutant core proteins, as compared to the $\beta$-galactosidase control protein. Thus, the various mechanisms potentially involved in core-induced steatosis, including

lipogenic gene expression [13–16], the modulation of lipogenic protein functions [17, 18], and effects on mitochondrial oxidative function [19–21] may also potentially be induced by an uncleaved HCV core protein. Both mature and immature core proteins have been shown to be involved in upregulation of the fatty acid synthetase (FAS) gene promoter [39]. Our results suggest that the change in the distribution of lipid droplets observed in cells producing the mature core protein is not due simply to the redistribution of the pre-existing droplets. This redistribution seems instead to be associated with the synthesis of new lipid droplets, due to the direct lipogenic effects of the HCV core protein. Further support for this interpretation is also provided by our 3D reconstructions of whole cells producing the mature core protein. These 3D reconstructions show that clusters of lipid droplets do not specifically arise close to the centrosome. The precise localisation of the lipid droplets clusters and centrosomes possible with this EM approach and the use of serial ultrathin sections is not consistent with the formation of these clusters by the simple migration of pre-existing droplets towards the centrosome. Again, our 3D EM analysis is more consistent with the de novo synthesis of lipid droplets at the site of cluster formation.

It remains unclear how triglycerides and other neutral lipids are packaged into cytosolic droplets. Several hypotheses have been proposed concerning nascent lipid droplet formation [39–42]. According to the most widely supported of these hypotheses, lipids accumulate between the two leaflets of the ER membrane, gradually taking on a globular shape and then being pinched off from the ER to become independent lipid droplets surrounded by a single, ER-derived, monolayer membrane [40–43]. However, neither nascent lipid droplets nor lipid deposition in the ER membrane has ever been visualised, due to technical constraints and the extremely rapid nature of this phenomenon, which takes place over the course of a few minutes [44]. Nevertheless, it has been suggested that the proteins of the PAT (perilipin-adipophilin-Tip47) family, which coat the lipid droplets, may be involved in this mechanism [45]. All PAT proteins have similar sequences and can bind to the surface of intracellular lipid droplets, either constitutively or in response to metabolic stimuli, such as an increased in lipid flux into or out of lipid droplets [46]. Each PAT protein has a unique tissue distribution, subcellular localisation and lipid-binding properties consistent with each of these proteins playing a unique role in triglyceride management [47]. These proteins are exchangeable at the surface of the lipid droplets in various conditions, and these exchanges regulate the storage of lipids within the cell [45, 46]. It has been suggested that PAT family proteins not only coat the droplets but actually order triglyceride packaging, by managing the interface between the droplet

and the cytosol and contributing to membrane curvature and the pinching off of the lipid droplet [45]. It has been shown that the mature HCV core displaces adipophilin from the surface of the lipid droplet [28]. Thus, in cells producing the mature HCV core protein, lipid droplets may emerge from the ER membranes in which the core protein is synthesised, due to a specific role of the mature core protein in lipid droplet morphogenesis. This may also explain how the HCV core protein replaces adipophilin at the surface of the lipid droplet. Immuno-EM observations, such as that shown for the mature/WT core protein in Fig. 2 support this model. Indeed, the lipid droplets seem to emerge from ER membranes rich in HCV core protein. Similar findings were obtained if the experiment was repeated and for large numbers of cells. It is indeed difficult to believe that lipid droplets dispersed throughout the cytoplasm would move specifically towards these areas with a core-rich ER membrane. It seems more likely that these lipid droplets surrounded by the HCV core protein bud from these specific ER domains enriched in core protein. So, what makes this phenomenon possible? Recent studies have suggested that lipid droplets are extremely dynamic organelles that may undergo repeated cycles of fusion and fission with the ER membrane, thereby accumulating or regressing within the confines of ER membranes [40, 41, 43, 47]. Lipids may then diffuse laterally in the ER towards the nascent lipid droplets [43]. This movement of lipid droplet may make it possible to deliver lipids to various membrane organelles in the cell for lipid exchange [48]. The fusion and fission of lipid droplets is probably favoured by the mobility of these organelles along the microtubule network [41, 48]. This could concern the radial, centrosome-attached microtubules and also the whole network of non-centrosomal microtubules. Thus, this mobility would account for the prevention of lipid droplet clustering in response to HCV core protein following disruption of the microtubule network or the microinjection of antibodies against motor proteins such as dynein [28].

Cells producing the WT/mature core protein contained larger amounts of lipid droplets than cells producing the immature/uncleaved mutant core protein. The reason for this difference is unknown, but it may be due to the ability of the mature core protein to localise at the surface of the lipid droplets, contributing to the morphogenesis of these organelles. Indeed, the overexpression of various members of the PAT family, such as adipophilin and perilipin, is associated with an expansion of the pool of lipid droplets within the cell [49–51]. The HCV mature core protein present at the surface of the lipid droplet may exert an additional effect through specific lipid interaction, increasing the number and/or size of lipid droplets within the cell, or by inducing the fusion of many small and

invisible lipid droplets forming large, more visible droplets. Alternatively, the mature core protein may induce a higher amount of triglyceride synthesis, as suggested by our intracellular triglyceride quantification. However, all these mechanisms may act together to induce the accumulation of lipid droplets in clusters seen in cells producing the WT HCV core protein, the fusion of nascent or existing lipid droplets to form larger droplets remaining a matter of debate [52].

In conclusion, we have shown that the clustering of lipid droplets induced by the HCV core protein does not result from a simple redistribution of pre-existing organelles. Instead, the HCV core protein seems to induce the de novo synthesis of lipid droplets in the perinuclear area of the cell. These results provide some insight into how HCV "hijacks" these organelles for its own life cycle. They also shed light on the mechanisms of lipid droplet morphogenesis and dynamic, which have remained poorly understood. Furthermore, our study demonstrates that the formation of these clusters by the HCV core protein is associated with a major increase in the cumulative area covered by lipid droplets. This increase may be due to the intrinsic properties of the core protein (mature or immature) and its interaction with various molecules involved in the lipid metabolism, but may also be due in part to the ability of the mature core protein to coat the nascent lipid droplets. These results should help to guide future studies of the mechanisms involved in the pathogenesis of HCV-induced liver steatosis.

## References

1. Alter MJ, Mast EE, Moyer LA, Margolis HS (1998) Hepatitis C. Infect Dis Clin North Am 12:13–26
2. Asselah T, Rubbia-Brandt L, Marcellin P, Negro F (2006) Steatosis in chronic hepatitis C: why does it really matter? Gut 55:123–130
3. Adinolfi LE, Gambardella M, Andreana A, Tripodi MF, Utili R, Ruggiero G (2001) Steatosis accelerates the progression of liver damage of chronic hepatitis C patients and correlates with specific HCV genotype and visceral obesity. Hepatology 33:1358–1364
4. Rubbia-Brandt L, Fabris P, Paganin S, Leandro G, Male PJ, Giostra E, Carlotto A, Bozzola L, Smedile A, Negro F (2004) Steatosis affects chronic hepatitis C progression in a genotype-specific way. Gut 53:406–412
5. Goodman ZD, Ishak KG (1995) Histopathology of hepatitis C virus infection. Semin Liver Dis 15:70–81
6. Monto A, Alonzo J, Watson JJ, Grunfeld C, Wright TL (2002) Steatosis in chronic hepatitis C: relative contributions of obesity, diabetes mellitus, and alcohol. Hepatology 36:729–736
7. Castera L, Hezode C, Roudot-Thoraval F, Lonjon I, Zafrani ES, Pawlotsky JM, Dhumeaux D (2004) Effect of antiviral treatment on evolution of liver steatosis in patients with chronic hepatitis C: indirect evidence of a role of hepatitis C virus genotype 3 in steatosis. Gut 53:420–424
8. Kumar D, Farrell GC, Fung C, George J (2002) Hepatitis C virus genotype 3 is cytopathic to hepatocytes: reversal of hepatic steatosis after sustained therapeutic response. Hepatology 36:1266–1272
9. Poynard T, Ratziu V, McHutchison J, Manns M, Goodman Z, Zeuzem S, Younossi Z, Albrecht J (2003) Effect of treatment with peginterferon or interferon alfa-2b and ribavirin on steatosis in patients infected with hepatitis C. Hepatology 38:75–85
10. Moradpour D, Penin F, Rice CM (2007) Replication of hepatitis C virus. Nat Rev Microbiol 5:453–463
11. Moriya K, Yotsuyanagi H, Shintani Y, Fujie H, Ishibashi K, Matsuura Y, Miyamura T, Koike K (1997) Hepatitis C virus core protein induces hepatic steatosis in transgenic mice. J Gen Virol 78:1527–1531
12. Moriya K, Fujie H, Shintani Y, Yotsuyanagi H, Tsutsumi T, Ishibashi K, Matsuura Y, Kimura S, Miyamura T, Koike K (1998) The core protein of hepatitis C virus induces hepatocellular carcinoma in transgenic mice. Nat Med 4:1065–1067
13. Dharancy S, Malapel M, Perlemuter G, Roskams T, Cheng Y, Dubuquoy L, Podevin P, Conti F, Canva V, Philippe D, Gambiez L, Mathurin P, Paris JC, Schoonjans K, Calmus Y, Pol S, Auwerx J, Desreumaux P (2005) Impaired expression of the peroxisome proliferator-activated receptor alpha during hepatitis C virus infection. Gastroenterology 128:334–342
14. Tanaka N, Moriya K, Kiyosawa K, Koike K, Gonzalez FJ, Aoyama T (2008) PPARalpha activation is essential for HCV core protein-induced hepatic steatosis and hepatocellular carcinoma in mice. J Clin Invest 118:683–694
15. Waris G, Felmlee DJ, Negro F, Siddiqui A (2007) Hepatitis C virus induces proteolytic cleavage of sterol regulatory element binding proteins and stimulates their phosphorylation via oxidative stress. J Virol 81:8122–8130
16. Kim KH, Hong SP, Kim K, Park MJ, Kim KJ, Cheong J (2007) HCV core protein induces hepatic lipid accumulation by activating SREBP1 and PPARgamma. Biochem Biophys Res Commun 355:883–888
17. Yamaguchi A, Tazuma S, Nishioka T, Ohishi W, Hyogo H, Nomura S, Chayama K (2005) Hepatitis C virus core protein modulates fatty acid metabolism and thereby causes lipid accumulation in the liver. Dig Dis Sci 50:1361–1371
18. Perlemuter G, Sabile A, Letteron P, Vona G, Topilco A, Chretien Y, Koike K, Pessayre D, Chapman J, Barba G, Brechot C. Hepatitis C virus core protein inhibits microsomal triglyceride transfer protein activity and very low density lipoprotein secretion: a model of viral-related steatosis. FASEB J 16: 185-194
19. Okuda M, Li K, Beard MR, Showalter LA, Scholle F, Lemon SM, Weinman SA (2002) Mitochondrial injury, oxidative stress, and antioxidant gene expression are induced by hepatitis C virus core protein. Gastroenterology 122:366–375
20. Korenaga M, Wang T, Li Y, Showalter LA, Chan T, Sun J, Weinman SA (2005) Hepatitis C virus core protein inhibits mitochondrial electron transport and increases reactive oxygen species (ROS) production. J Biol Chem 280:37481–37488
21. Machida K, Cheng KT, Lai CK, Jeng KS, Sung VM, Lai MM (2006) Hepatitis C virus triggers mitochondrial permeability

transition with production of reactive oxygen species, leading to DNA damage and STAT3 activation. J Virol 80:7199–7207

22. Moradpour D, Englert C, Wakita T, Wands JR (1996) Characterization of cell lines allowing tightly regulated expression of hepatitis C virus core protein. Virology 222:51–63

23. Barba G, Harper F, Harada T, Kohara M, Goulinet S, Matsuura Y, Eder G, Schaff Z, Chapman MJ, Miyamura T, Brechot C (1997) Hepatitis C virus core protein shows a cytoplasmic localization and associates to cellular lipid storage droplets. Proc Natl Acad Sci USA 94:1200–1205

24. Hope RG, McLauchlan J (2000) Sequence motifs required for lipid droplet association and protein stability are unique to the hepatitis C virus core protein. J Gen Virol 81:1913–1925

25. Shi ST, Polyak SJ, Tu H, Taylor DR, Gretch DR, Lai MM (2002) Hepatitis C virus NS5a colocalizes with the core protein on lipid droplets and interacts with apolipoproteins. Virology 292:198–210

26. Roingeard P, Hourioux C (2008) Hepatitis C virus core protein, lipid droplets and steatosis. J Viral Hepat 15:157–164

27. Miyanari Y, Atsuzawa K, Usuda N, Watashi K, Hishiki T, Zayas M, Bartenschlager R, Wakita T, Hijikata M, Shimotohno K (2007) The lipid droplet is an important organelle for hepatitis C virus production. Nat Cell Biol 9:1089–1097

28. Boulant S, Douglas MW, Moody L, Budkowska A, Targett-Adams P, McLauchlan J (2008) Hepatitis C virus core protein induces lipid droplet redistribution in a microtubule and dynein-dependent manner. Traffic 9:1268–1282

29. McLauchlan J, Lemberg MK, Hope G, Martoglio B (2002) Intramembrane proteolysis promotes trafficking of hepatitis C virus core protein to lipid droplets. EMBO J 21:3980–3988

30. Hourioux C, Patient R, Morin A, Blanchard E, Moreau A, Trassard S, Giraudeau B, Roingeard P (2007) The genotype 3-specific hepatitis C virus core protein residue phenylalanine 164 increases steatosis in an in vitro cellular model. Gut 56:1302–1308

31. Blanchard E, Brand D, Trassard S, Goudeau A, Roingeard P (2002) Hepatitis C virus-like particle morphogenesis. J Virol 76:4073–4079

32. Blanchard E, Hourioux C, Brand D, Ait-Goughoulte M, Moreau A, Trassard S, Sizaret PY, Dubois F, Roingeard P (2003) Hepatitis C virus-like particle budding: role of the core protein and importance of its Asp111. J Virol 77:10131–10138

33. Ait-Goughoulte M, Hourioux C, Patient R, Trassard S, Brand D, Roingeard P (2006) Core protein cleavage by signal peptide peptidase is required for hepatitis C virus-like particle assembly. J Gen Virol 87:855–860

34. Folch J, Lees M, Sloane-Stanley GH (1957) A simple method for the isolation and purification of total lipids from animal tissues. J Biol Chem 226:497–509

35. Roingeard P, Hourioux C, Blanchard E, Prensier G (2008) Hepatitis C virus budding at lipid droplet-associated ER membrane visualized by 3D electron microscopy. Histochem Cell Biol 130:561–566

36. Kremer JR, Mastronarde DN, McIntosh JR (1996) Computer visualization of three-dimensional image data using IMOD. J Struct Biol 116:71–76

37. Ai LS, Lee YW, Chen SS (2009) Characterization of hepatitis C virus core protein multimerization and membrane envelopment: revelation of a cascade of core-membrane interactions. J Virol 83:9923–9939

38. Kasurinen J (1992) A novel fluorescent fatty acid, 5-methyl-bdy-3-dodecanoic acid, is a potential probe in lipid transport studies by incorporating selectively to lipid classes of BHK cells. Biochem Biophys Res Commun 187:1594–1601

39. Jackel-Cram C, Babiuk LA, Qiang L (2007) Up-regulation of fatty acid synthase promoter by hepatitis C virus core protein: genotype-3a core has a stronger effect than genotype-1b core. J Hepatol 6:999–1008

40. Ohsaki Y, Cheng J, Suzuki M, Shinohara Y, Fujita A, Fujimoto T (2009) Biogenesis of cytoplasmic lipid droplets: from the lipid ester globule in the membrane to the visible structure. Biochim Biophys Acta 1791:399–407

41. Fujimoto T, Ohsaki Y, Cheng J, Suzuki M, Shinohara Y (2008) Lipid droplets: a classic organelle with new outfits. Histochem Cell Biol 130:263–279

42. Thiele C, Spandl J (2008) Cell biology of lipid droplets. Curr Opin Cell Biol 20:378–385

43. Walther TC, Farese RV Jr (2009) The life of lipid droplets. Biochim Biophys Acta 1791:459–466

44. Kuerschner L, Moessinger C, Thiele C (2008) Imaging of lipid biosynthesis: how a neutral lipid enters lipid droplets. Traffic 9:338–352

45. Wolins NE, Brasaemle DL, Bickel PE (2006) A proposed model of fat packaging by exchangeable lipid droplet proteins. FEBS Lett 580:5484–5491

46. Bickel PE, Tansey JT, Welte MA (2009) PAT proteins, an ancient family of lipid droplet proteins that regulate cellular lipid stores. Biochim Biophys Acta 1791:419–440

47. Goodman JM (2008) The gregarious lipid droplet. J Biol Chem 283:28005–28009

48. Zehmer JK, Huang Y, Peng G, Pu J, Anderson RG, Liu P (2009) A role for lipid droplets in inter-membrane lipid traffic. Proteomics 9:914–921

49. Imamura M, Inoguchi T, Ikuyama S, Taniguchi S, Kobayashi K, Nakashima N, Nawata H (2002) ADRP stimulates lipid accumulation and lipid droplet formation in murine fibroblasts. Am J Physiol Endocrinol Metab 283:775–783

50. Fukushima M, Enjoji M, Kohjima M, Sugimoto R, Ohta S, Kotoh K, Kuniyoshi M, Kobayashi K, Imamura M, Inoguchi T, Nakamuta M, Nawata H (2005) Adipose differentiation related protein induces lipid accumulation and lipid droplet formation in hepatic stellate cells. In Vitro Cell Dev Biol Anim 41:321–324

51. Listenberger LL, Ostermeyer-Fay AG, Goldberg EB, Brown WJ, Brown DA (2007) Adipocyte differentiation-related protein reduces the lipid droplet association of adipose triglyceride lipase and slows triacylglycerol turnover. J Lipid Res 48:2751–2761

52. Cheng J, Fujita A, Ohsaki Y, Suzuki M, Shinohara Y, Fujimoto T (2010) Quantitative electron microscopy shows uniform incorporation of triglycerides into existing lipid droplets. Histochem Cell Biol 132:281–291